Laser Interferometer Systems for Precise Measurements of Ground-Strains

AUTHOR(S):

TAKEMOTO, Shuzo

CITATION:

TAKEMOTO, Shuzo. Laser Interferometer Systems for Precise Measurements of Ground-Strains. Bulletin of the Disaster Prevention Research Institute 1979, 29(2): 65-81

ISSUE DATE:

1979-08

URL:

http://hdl.handle.net/2433/124884

Laser Interferometer Systems for Precise Measurements of Ground-Strains

By Shuzo TAKEMOTO

(Manuscript received July 5, 1979)

Abstract

Four extensometers with laser interferometer systems were installed and have been successively operated in the tunnel at the Amagase Crustal Movement Observatory.

Two of them (EL–1 and EL–V) are super-invar bar extensometers with laser interferometer systems consisting of simple laser sources, Michelson interferometers and photodetecting equipment with image-sensors. The remaining two components (L–1 and L–2) are laser extensometers with a frequency-stabilized laser source.

Using long term continuous records obtained from EL–1 and L–1, which are orientated along the same direction, effects of instrumental and environmental disturbances have been investigated.

Secular ground-strains observed with both components are inconsistent with each other. This disagreement is considered to be mainly caused by the effect of slowly increasing pressure in the enclosing pipes of L–1.

Non-periodic ground-strains (residual strains obtained by subtracting the mean values of long term drifts and tidal constituents from observed data of EL–1 and L–1) are consistent with each other in the amplitude range of larger than 10^{-8}. But they are inconsistent in the amplitude range of smaller than 10^{-8} because of different effects of instrumental and environmental disturbances.

Tidal strain amplitudes obtained from EL–1 are about 27% smaller than those obtained from L–1. The former may be diminished by frictional forces between the super-invar bar and its supporting rollers.

1. Introduction

Extensometers, employing length standards in forms of quartz tubes or super-invar bars, have been commonly used for measurements of ground-strains in many observatories.

Until recently, the precision of measurement with these extensometers was not discussed so much quantitatively because of difficulties in absolute calibration. But if we want to carry out a quantitative investigation of ground-strains of the order of 10^{-8}, we cannot do it without absolute calibration of instruments in this amplitude range.

For instance, together with tidal strains of the order of 10^{-8}, relative displacements between the fixed and free ends of an extensometer having a length of 10 m are found to be 1 μm or so. For the absolute calibration of instruments in this amplitude range, the use of interferometry is considered to be most effective. Because displacements as small as 1 μm can be measured quantitatively in terms of the wavelength of a light. Some

calibration systems with interferometers have been developed (Blayney et al.[1]; Hade et al.[2]; Smookler et al.[3]).

In the disused race tunnel at the Amagase Crustal Movement Observatory (34°53'N, 135°50'E, H=70.3 m), a laser interferometer system, which is similar to that described by Hade et al.[2], has been used for the absolute calibration of the roller type super-invar bar extensometer (Takemoto[4],[5]). This system consists of a Michelson interferometer with a simple Helium-Neon gas laser and a piece of photo-detecting equipment with an image-sensor. Calibration signals are given by means of heating the super-invar bar and resultant displacements of about 4~7 μm are recorded with the interferometer system and the photographic recording system. Comparing both records, it was found that displacements obtained from the photographic recording system are far smaller than those obtained from the interferometer system; the former are about 35~60% of the latter in the amplitude range of 1~3 μm. This discrepancy is considered to be due to the frictional force between the super-invar bar and the roller.

This laser interferometer system, developed for the calibration of the roller type super-invar bar extensometers, can be also used for obtaining long term continuous records of ground-strains with high resolution. Therefore, these systems were attached to two components out of the seven super-invar bar extensometers installed at Amagase. One component is orientated along the tunnel and has a length of 40.0 m (EL-1). The other one is a vertical component having a length of 5.6 m (EL-V). These systems can be characterized as "laser extensometers with length standards of rigid bars".

On the other hand, "laser extensometers with length standards of light beams" have been developed by a number of groups (Van Veen et al.[6]; Vali et al.[7]; Berger and Rovberg[8]; Levine and Hall[9]; Goulty et al.[10]). The advantage of these extensometers is to be free from some troubles inherent in conventional ones with "length standards of rigid bars", i.e. it is not necessary to consider effects from the frictional forces between "length standards" and their supports and the deformations of "length standards" themselves.

However, in order to measure the ground-strain to 1 in 10^8 with a laser extensometer of this type, it is necessary that the frequency of the laser, in terms of which the ground-strain is measured, should be constant to better than 1 in 10^8. The frequency-stability of a simple laser is determined to be about 1 in 10^6 and it is not enough to construct a laser extensometer of this type. Various schemes for stabilizing the frequency of a laser have been deviced. For instance, Berger and Lovberg[8] stabilized the frequency of the Helium-Neon gas laser operating at 6328 Angstroms with an external resonator consisting of a pair of mirrors and an annealed quartz tube having a length of 30 cm. The frequency-stability of this system was estimated to be 1.5×10^{-9} during the laser life-time.

In our case, a frequency-stabilized laser (Model HP 5501A), manufactured by Hewlett-Packard Inc., was used for the construction of "laser extensometers with length standards of light beams".

Using this laser, the stability of which was determined to be better than 10^{-8}, two

components of laser extensometers of this type were installed in the same tunnel at Amagase (L–1 and L–2).

In this paper, both types of laser extensometer systems which have successively operated at Amagase, are described in the first part. In the second part, relative performance of the two components, which are different in type but are orientated along the same direction, is discussed.

2. Description of Instruments

2.1 Super-Invar Bar Extensometer with a Laser Interferometer

The installation of laser extensometers, together with the topographic profile along the observational tunnel, is shown in Fig. 1. EL–1 and EL–V show super-invar bar extensometers with laser interferometers. The former is a horizontal component orientated along the tunnel (N 72.5°W) and the latter is a vertical component.

The block diagram and time chart are shown in Fig. 2. One of the reflecting mirrors in the Michelson interferometer is mounted at the free end of the super-invar bar and the other is fixed to the concrete pier. The fringe displacement in the interference pattern, formed by the relative displacement of two reflecting mirrors, is detected photo-electrically by an image-sensor consisting of a row of 64 photodiodes spaced on 50.8 μm centers, with a 40.6 μm $\times$ 50.8 μm aperture. Access to the diodes is made in

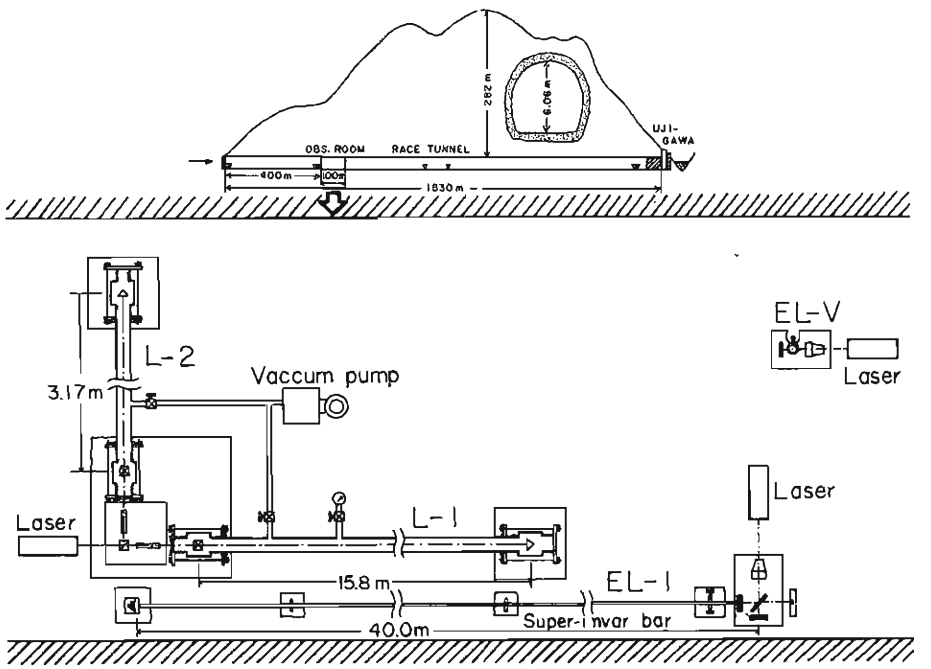

Fig. 1. Topographic profile along disused race tunnel (upper) and installations of laser extensometers in the observation room (lower).

sequence by a shift register which is driven by an external clock signal consisting of a pulse-train of 65.536 kHz. A start pulse, which is required to initiate each scan, is also supplied externally at a sequence of 512 Hz. When each diode is accessed, it is

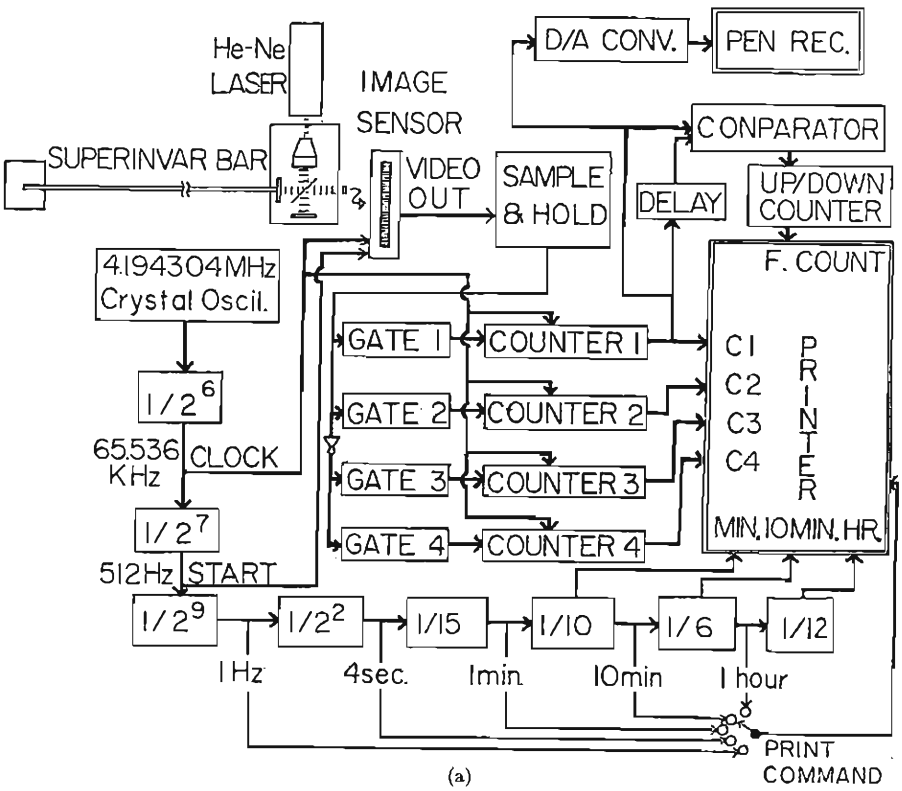

Fig. 2. Block diagram and time chart of recording system of extensometer with a laser interferometer.

charged through a common video line. And so, the signal which appears on the video line is a train of 64 charged pulses having a magnitude proportional to the light intensity on each photodiode. This signal is fed to the four gate circuits (Gate 1∼4) through an amplifier and a sample-and-hold circuit which produces "square waves". The high or low level of the sample-and-hold signal respectively corresponds to the bright or dark fringe in the interference pattern.

Gate 1 and Gate 3 are set to be opened at the positive-going edge of the start pulse and Gate 1 is closed at the high-to-low transition of the sample-and-hold output and Gate 3 is closed at the low-to-high transition of this output. Gate 2 (Gate 4) is opened at the first high-to-low (low-to-high) transition of the sample-and-hold output and is closed at the second high-to-low (low-to-high) transition of this output. Clock pulses are applied through Gate 1∼4 to the four counters (C–1∼4). The output of C–1 (C–3) is proportional to the displacement of the bright (dark) fringe in the interference pattern and the output of C–2 (C–4) corresponds to the interval between two adjacent bright (dark) fringes. This interval depends on the angle of relative inclination between two reflecting mirrors, therefore, by means of slightly turning one of mirrors, it can be adjusted to be about 1.5 mm at the surface of the image-sensor. As a result, the numerical values counted by C–2 or C–4 is about 30, and the least count of C–1 or C–3 corresponds to one-thirtieth of the interval between two adjacent fringes (i.e. one-sixtieth of the wavelength). For the light source of this interferometer system, we use a simple Helium-Neon gas laser operating at a wavelength of 6328 Angstroms (=0.6328 μm), and so the resolving power of this system for the ground-strain measurement is about 1×10^{-8}/L (m), where L is the standard length of the super-invar bar. Thus,

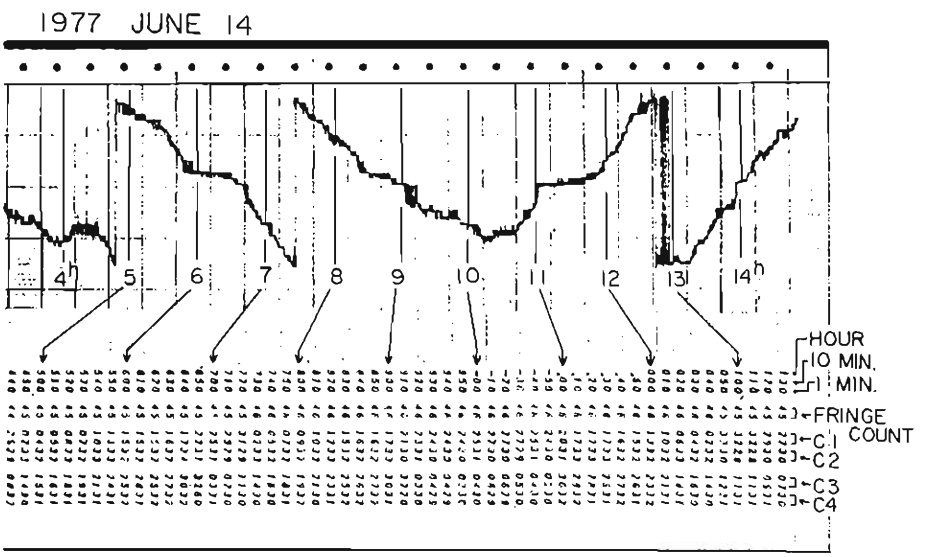

Fig. 3. Actual records of EL–1 component: upper; analog record, lower; digital record.

EL-1 and EL-V are able to measure ground-strains of 2.5×10^{-10} and 1.8×10^{-9}, respectively.

When the relative displacement between two reflecting mirrors becomes equal to half a wavelength ($=0.3164\,\mu$m), each fringe is replaced by its neighbor and a step discontinuity appears on records of C-1 and C-3. These discontinuities are also counted with a reversible counter and printed out on the recording paper, together with outputs from C-1$\sim$4.

The digital output from C-1 is applied to the digital-to-analog converter and the analog output voltage is recorded on a chart recorder. Examples of the digital and analog records of this system are shown in Fig. 3.

The clock pulse, start pulse and printer-controlling pulses in this system are provided by a crystal oscillator of 4.194304 MHz.

2.2 Laser Extensometer with a Frequency-Stabilized Laser

L-1 and L-2, shown in Fig. 1, consist of the HP 5501A laser transducer system and evacuated light paths. The laser transducer head of this system is a frequency-stabilized Helium-Neon gas laser with the Zeeman frequency split beam which is produced by an axial magnetic field. The frequency split is about 2×10^6 Hz, relative to the laser frequency of 5×10^{14} Hz. One frequency component (f_1) is polarized vertically and the other one (f_2) horizontally. The light beam, passing out of the laser head, is split at the surface of a 50% beam splitter, which deflects half of the beam at the right angle and passes the remaining half. Each of two beams, used for two orthogonal interferometers, is split again at the surface of a polarized beam splitter. One frequency component (f_1) is transmitted to the retro-reflecting corner cube mirror and the other one (f_2) is reflected to the reference corner cube mirror mounted on the polarized beam splitter housing. Both frequency components are reflected back to the photodetector in the receiver. The relative displacement between the retro-reflecting and reference corner cube mirrors causes a Doppler shift in the frequency component (f_1). The difference between frequency component (f_2) and the Doppler shifted one ($f_1\pm\Delta f_1$) is detected by the receiver. This Doppler shifted difference frequency forms the "measurement signal". On the other hand, the "reference signal" (f_2–f_1) is provided from the laser head. The HP 10670 counter accessory receives the measurement and reference signals and compares them cycle-by-cycle in a dual output mixer. The mixer produces an appropriate up or down output pulse whenever one of the signals gets one-half cycle ahead of or behind the other. Each pulse corresponds to the one-quarter wave length ($=0.158\,\mu$m) in "normal resolution" and one-fortieth wave length ($=0.0158\,\mu$m) in "extended resolution". In our case, "extended resolution" is used for pulse accumulations in the reversible counter.

The output from the counter is printed out on the recording paper. And also, this digital output is converted with a digital-to-analog converter and the analog output voltage is recorded on a 12 point dotting recorder.

L-1 and L-2 have lengths of 15.8 m and 3.2 m, respectively. Thus, the resolving

powers of these extensometers for ground-strain measurements are 1×10^{-9}/digit and 5×10^{-9}/digit, respectively. But the frequency-stability of the HP 5501A laser is estimated to be about 1 in 10^8 and so accuracies of these systems for ground-strain measurements are also estimated to be about 1×10^{-8}. This can be examined in cases of electricity failures, when the temperature in the laser head is suddenly changed and the frequency servo control system is repeatedly operated. Fig. 4 shows analog voltage outputs of L–1 and L–2 recorded on the dotting recorder in such cases. Electricity failures occurred twice in September 27 1978, and accordingly, the record of L–1 fluctuated by about 10 digits and that of L–2 by 2∼3 digits. These fluctuations corresponded to 1×10^{-8} and they were within the limits of the laser frequency fluctuation.

The light paths of two laser interferometers (L–1 and L–2) were enclosed independently in stainless steel pipes and double bellows chambers which were essentially similar to ones employed by Goulty et al.[10]. By using push-pull bellows no stress can be transmitted between the optical components via the enclosing pipes. The pipe sections were jointed together with flanges and O-ring-seals at 2∼3 m intervals. Each of the pipes has a diameter of 48 mm and a thickness of 3 mm. Enclosing pipes were evacuated by a conventional mechanical pump with a capacity of 315 liters per minute.

Generally, as shown by Goulty et al.[10], vacuum pumps have been operated continuously and the pressure in enclosing pipes of interferometers has been kept at 10^{-2} torr or less. But in our case, the vacuum pump was only used at the start to make a vacuum of 10^{-3} torr, and after that, it was not used because its continuous operation

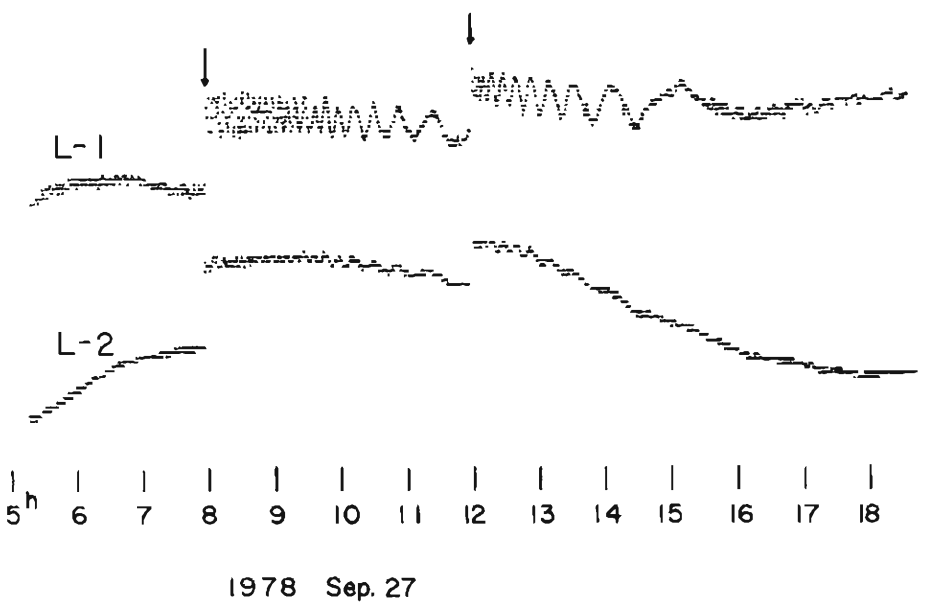

Fig. 4. Examples of records of L–1 and L–2 components at times when electric power supply was interrupted.

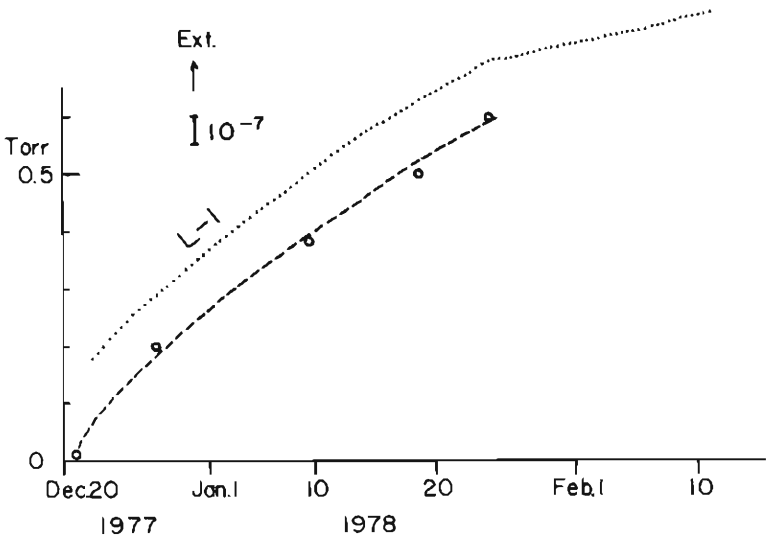

Fig. 5. Relative changes of ground-strain obtained from L–1 and pressure in the enclosing apparatus.

causes some disturbances for other instruments installed in the same observation room.

Fig. 5 shows changes of the pressure in the enclosing pipes and the ground-strain accumulation observed with L–1 for the period from Dec. 20 1977 to Feb. 12 1978. The vacuum pump was operated on Dec. 20 1977. The pressure was measured with a vacuum gauge of the Mackleod type and a Geissler tube. The valve isolating the evacuated enclosing pipes from the vacuum gauge of the Mackleod type was shut off on Jan. 24 1978.

During the period from Dec. 20 1977 to Jan. 24 1978, the change of the ground-strain was proportional to that of the pressure in the enclosing pipes. After Jan. 24 1978, when the valve was shut off, the rate of ground-strain accumulation obviously decreased. Thus, it is reasonable to consider that the "apparent" secular ground-strain observed with L–1 is caused by the pressure change in the enclosing pipes and does not correspond to the "true" secular ground-strain.

3. Comparison of Two Laser Extensometers of Different Designs

Two types of laser extensometers, described in the previous paragraph, were installed in the same co-axial direction along the tunnel (Fig. 1). One, EL–1, using a 40 m super-invar bar as a length standard, has been successively operated since May 1977, and the other, L–1, using a stabilized laser light beam as a length standard, has been operated since June 1977. Examples of records, obtained from these two extensometers for a period of a fortnight, are shown in Fig. 6, together with barometric and thermometric records obtained in the same observation room.

Some characteristic features may be seen in this figure; (1) EL–1 and L–1 are

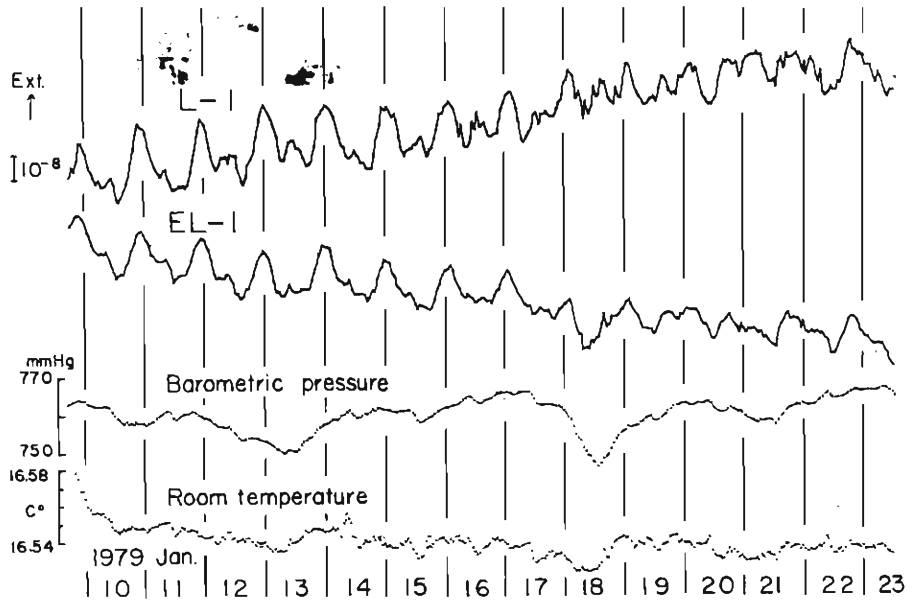

Fig. 6. Examples of records of L–1 and EL–1 components, together with thermometric and barometric records for a period of a fortnight.

drifting apart in opposite directions; (2) the amplitude of tidal strain obtained from EL–1 is smaller than that obtained from L–1; (3) non-periodic ground-strains having amplitudes of 10^{-8} or less are inconsistent with each other.

More detailed discussions on these points are described in the following three sections with 156-days of continuous data obtained from EL–1 and L–1.

3.1 Secular Ground-Strain

Secular ground-strains, which are shown in Fig. 7, were obtained from continuous records of EL–1 and L–1 for the period from Jul. 8 to Dec. 12 1978. In this case, tidal strain constituents were eliminated with the Pertzev's filter[11].

The strain accumulation obtained from EL–1 for this period exhibited a contraction of about 5.5×10^{-7}. On the contrary, that obtained from L–1 exhibited an extension of about 7×10^{-7}. This discrepancy is considered to be mainly due to the "apparent" extension of L–1 caused by slowly increasing pressure in the enclosing pipes of the interferometer system.

The strain accumulation obtained from EL–1 is consistent with the data obtained from electro-optical distance measurements of three base-lines in the same tunnel at Amagase. These measurements with a Geodimeter Model 6 have been repeatedly made since 1968 and strain accumulations of three base-lines having lengths of 700～1700 m exhibited contracting rates of $2.6\sim1.5\times10^{-6}$/year for the period from 1968 to 1977 (Furuzawa et al.[12]).

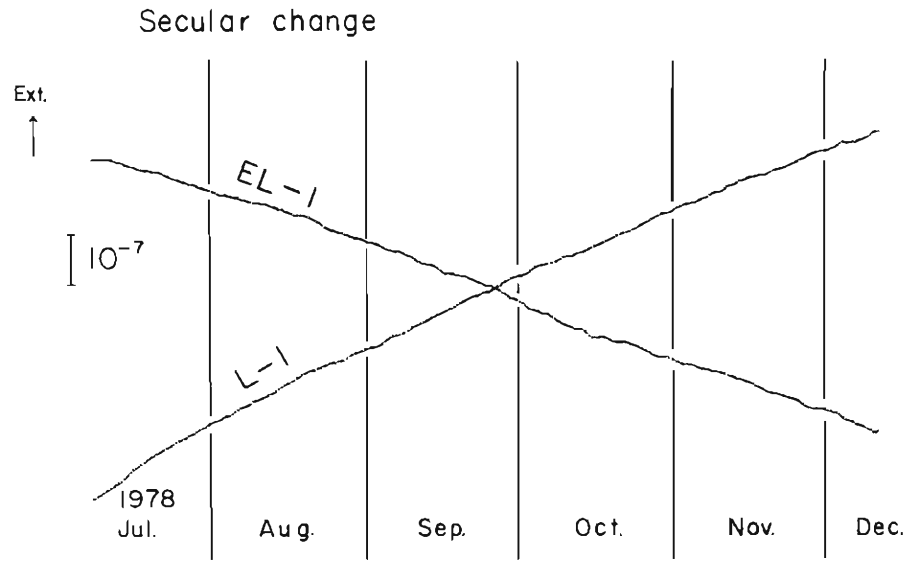

Fig. 7. Secular changes obtained from EL–1 and L–1.

3.2 Residual Strain Obtained by Subtracting the Mean Value of Long Term Drift from Observed Secular Ground-Strain

In the previous section, secular ground-strains obtained from EL–1 and L–1 for a period of about five months were compared and as a result they were inconsistent with each other. In this section, we will discuss about residual strains which are obtained by subtracting mean values of long term drifts from observed ground-strains.

The secular ground-strain (zero-point drift) $e(t)$ is defined by

$$e(t)=Y(t)-\sum A_n \cos(\sigma_n-\delta_n) \tag{1}$$

where $Y(t)$ is the observed value of EL–1 or L–1.

As a first approximation, we assume the mean value ($\bar{e}_1$) of the long term drift to be a straight line, then

$$\bar{e}_1(t)=a\times t. \tag{2}$$

The coefficient a is determined by the least squares fitting of $e(t)$, then we obtain

$$a=(-3.514\pm 0.002)\times 10^{-9}/\text{day}$$

for EL–1, and

$$a=(4.452\pm 0.006)\times 10^{-9}/\text{day}$$

for L–1.

The residual strain $e_r(t)$ is defined by

$$e_r(t)=e(t)-\bar{e}_1(t) \tag{3}$$

and those of EL–1 and L–1 are shown in Fig. 8.

L–1 shows a convex feature as a whole. The following reason can be considered in this respect; the pressure change in the enclosing pipes of L–1 is not linear as time goes by, but it contains an exponentially decreasing term. Then, as a second approximation, we assume the following equation for the mean value of the long term drift of L–1,

$$\bar{e}_2(t)=\alpha\times t+\beta(1-\exp(-\gamma t)) \tag{4}$$

where $\alpha=4.05\times10^{-9}$/day, $\beta=8\times10^{-8}$ and $\gamma=0.0197$. The residual strain in this case is expressed by

$$e_r(t)=e(t)-\bar{e}_2(t). \tag{3}'$$

In Fig. 8, it is marked with L–1'. Both residual strains of EL–1 and L–1' are approximately consistent with each other in the amplitude range of larger than 10^{-8}.

But in the amplitude range of smaller than 10^{-8}, they are inconsistent. This can be explained as follows; the strain change of L–1 in this amplitude range are mainly caused by the fluctuation of the laser frequency, but as shown in Fig. 6 and Fig. 8, they are not affected by meteorological conditions such as the atmospheric pressure change in the observation room. On the contrary, the strain changes of EL–1 involve effects of meteorological disturbances. As shown in Fig. 6, non-periodic changes of ground-strains obtained from EL–1 correlate with temperature variations in the observation room. For temperature variations of 0.02°C, "apparent" ground-strains obtained from

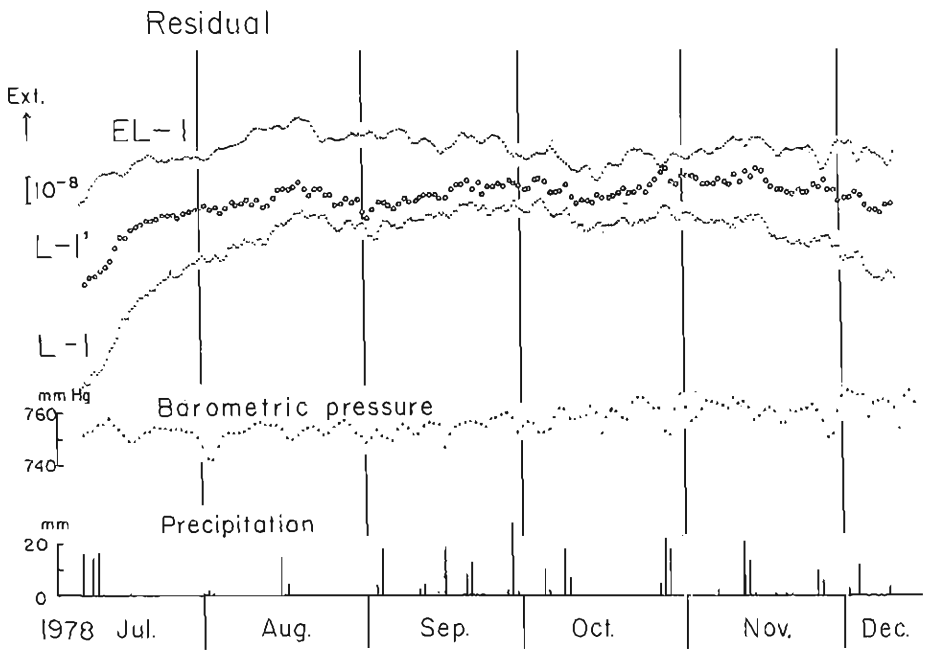

Fig. 8. Residual strains obtained from EL–1 and L–1, together with barometric pressure change and precipitation, where L–1' is a second approximation of L–1.

EL–1 exhibit some parts in 10^9. And these variations of the room temperature also correlate with the gradients of atmospheric pressure changes.

The similar consideration about meteorological disturbances was given by Sydenhan[13]. He concluded that adiabatic heating, due to pressure changes, caused a dominant effect on records of extensometers.

In this respect, more detailed discussions will be made in the future.

3.3 Tidal Strain

3.3.1 Comparison of Observed and Theoretically Predicted Tidal Strains

Using the same data of EL–1 and L–1, mentioned in the previous section, tidal strains were analyzed. Amplitudes and phases of nine major tidal constituents were determined by applying the least squares method to the drift-eliminated data for a period of 3740 hours.

Comparing amplitudes of nine constituents obtained from EL–1 with those obtained from L–1, there are systematic discrepancies between them; the former ones are about 27% smaller than the latter. These relations are shown in Fig. 9. The amplitude ratios between the results obtained from EL–1 and those obtained from L–1 are constant for all of tidal constituents, i.e. diurnal (K_1, J_1, M_1, O_1, Q_1), semi-diurnal (M_2, N_2, S_2) and

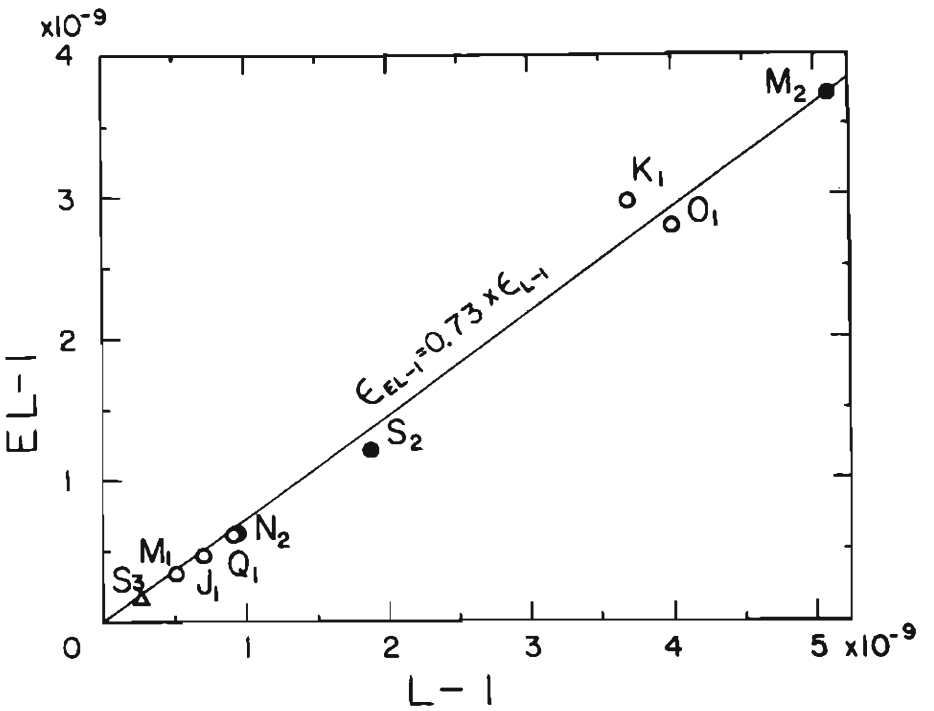

Fig. 9. Relative amplitudes of nine constituents of tidal strains obtained from EL–1 and L–1.

ter-diurnal (S_3) constituents.

Then, observed tidal strains of M_2 and O_1 constituents were compared with the theoretically predicted values, consisting of theoretical tidal strains for a solid earth (E) and contributions from loading effects of ocean tides (L). Love numbers (h=0.6114 and l=0.0832) were used for the calculation of theoretical tidal strains. The loading effects of ocean tides at the Amagase Observatory were calculated by convolving data of ocean tides with surface mass loading Green's functions obtained by Farrel[14] for the Gutenberg-Bullen A earth model.

In our calculations, the ocean tides were divided into two parts; local tides in the seas adjacent to Japan, and global tides in the rest of the world oceans. We adopted results obtained by Ogura[15] for the former part and co-tidal charts of the *ATAAC OKEAHOB*[16),17] for the latter part.

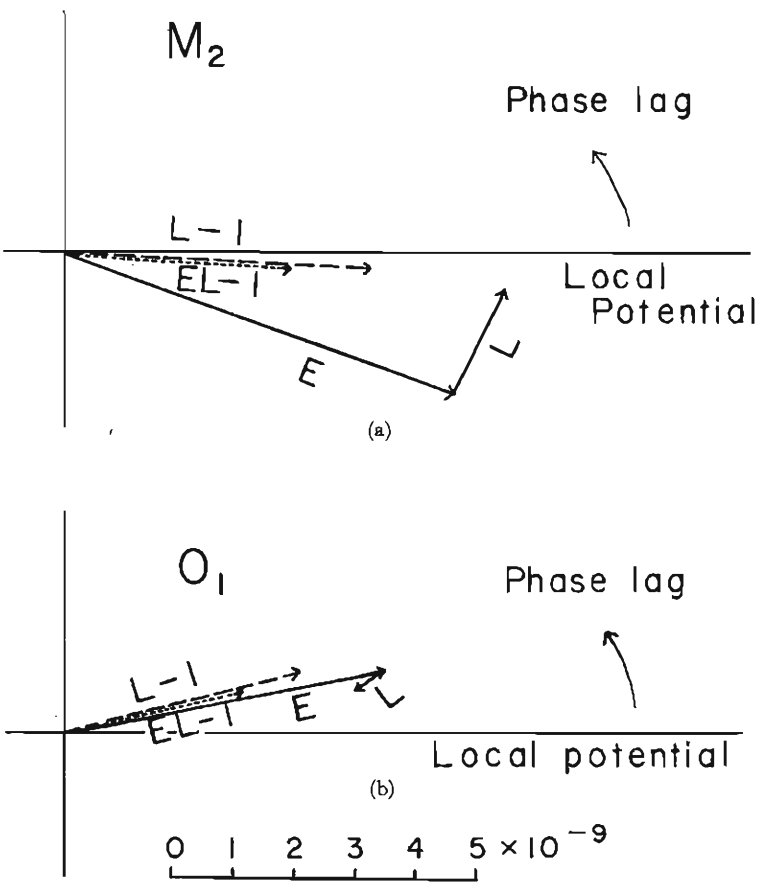

Fig. 10. Vector diagrams of M_3 and O_1 constituents: E; theoretically predicted value for a solid earth, L; contribution from ocean tide loading, EL-1; observed with EL-1 component, L-1; observed with L-1 component.

Table 1. Amplitudes and phase lags of M_2 and O_1 constituents

	M_2 constituent		O_1 constituent	
	Amplitude ($\times 10^{-9}$)	Phase lag (degree)	Amplitude ($\times 10^{-9}$)	Phase lag (degree)
Theoretical (N 72.5°W)				
Theoretical strain for a solid earth (E)	6.81	−19.6	5.39	11.0
Contribution from the ocean tide loading (L)	1.90	64.6	0.53	−148.1
Total ((E)+(L))	7.25	−4.5	4.89	8.9
Observed (N 72.5°W)				
L-1	5.10	−2.7	3.94	14.6
EL-1	3.70	−3.6	2.96	14.1

The observed and theoretically predicted tidal strains are shown as vectors in Fig. 10 and amplitudes and phases of these values are also shown in Table 1.

In both of M_2 and O_1 constituents, amplitudes of observed tidal strains are smaller than those of theoretically predicted ones. These differences may be explained by topographic and geological effects. But in any case, observed values of EL-1 are too small to be explained by these effects. We consider that the frictional forces between the super-invar bar and supporting rollers are the most possible source of these differences.

3.3.2 Temporal Variations of Tidal Strains

Temporal variations of tidal strain amplitudes were investigated by several authers in relation to the occurrences of major earthquakes and tectonic activities in fracture zones (Latynina and her co-workers[18),19),20)]; Mikumo et al.[21)]).

In this subsection, we discuss about temporal variations of M_2 and O_1 tidal strain amplitudes obtained from EL-1 and L-1. For these analyses, we used following two methods; the least squares method and the Pertzev's method (Pertzev[22)]). And they were applyed to the drift-eliminated data of EL-1 and L-1 for the sample time intervals of 696 hours. The 125 times analyses were successively repeated by shifting the time intervals to every 24 hours. Results are shown in Fig. 11. Tidal strain amplitudes obtained by the least squares method did not differ significantly from those obtained by Pertzev's method. Comparing results obtained from EL-1 with those from L-1, the relative changes between two time series of O_1 tidal strain amplitudes are consistent with each other, but in the case of M_2 constituent those are inconsistent. Therefore, we could not detect distinct variations appearing commonly on all of the time series.

4. Conclusions

Two types of laser extensometer systems have been described. These systems have been operated successively for a period of more than 1 year at the Amagase Crustal Movement Observatory.

One of them, a super-invar bar extensometer with a laser interferometer system, has

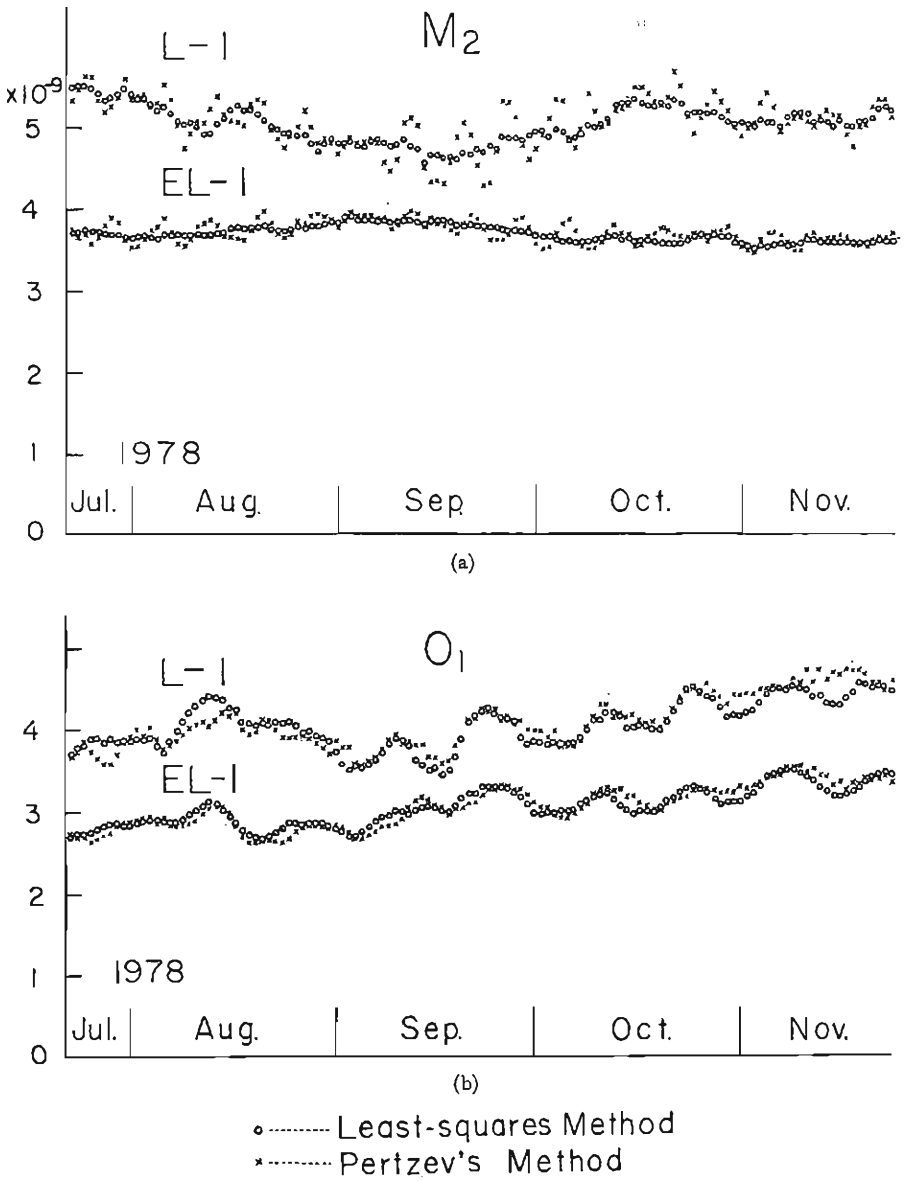

Fig. 11. Temporal variations of M_2 and O_1 tidal strain amplitudes obtained from EL-1 and L-1.

advantages of high resolution compared with conventional roller type extensometers and relative cheapness in construction, compared with laser extensometers with frequency-stabilized laser systems. But this instrument cannot be free from effects of frictional forces between the super-invar bar and supporting rollers.

On the other hand, a laser extensometer with a frequency-stabilized laser system is

not affected by such frictional forces. Therefore this system is suitable for the quantitative investigation of "strain steps" associated with earthquakes. This aspect we will discuss in subsequent papers.

Comparing records, obtained from both systems (EL–1; the former, L–1; the latter) orientated along the same direction, following results have been obtained.

(1) The secular ground-strain obtained from EL–1 exhibits the contraction of 5.5×10^{-7} for a period of 156-days. This result agrees with those obtained from electro-optical distance measurements of three base-lines in the same tunnel. This suggests that the data obtained from EL–1 is indicatable of the regional strain accumulation around Amagase. While, L–1 cannot be used for the measurement of secular ground-strains. Because it is disturbed by the slowly increasing pressure in its enclosing pipes.

(2) Non-periodic ground-strains obtained from both systems were consistent with each other in the amplitude range of larger than 10^{-8}. Investigations of these strains in relation to occurrences of major earthquakes will be made in the future. In the amplitude range of smaller than 10^{-8}, the record of EL–1 is disturbed by meteorological conditions, especially by temperature variations of the observation room. While, disturbances of L–1 in this amplitude range are mainly caused by the fluctuation of the laser frequency.

(3) Periodic tidal strains were analyzed with records of 3740 hours. In these long term analyses, effects of non-periodic noises, described above, were negligible. Comparing amplitudes of nine major constituents, there are systematic discrepancies between the results of EL–1 and those of L–1, i.e. the former are about 27% smaller than the latter. It can be considered that ground-strains obtained from EL–1 may be diminished by frictional forces between the super-invar bar and supporting rollers in the tidal strain amplitude range.

Temporal variations of M_2 and O_1 constituents were also investigated preliminarily. But distinct variations which should appear on all time series obtained from EL–1 and L–1 were not observed.

Acknowledgements

The author wishes to express his sincere thanks to Prof. Michio Takada and Dr. Tamotsu Furuzawa for their encouragement and helpful suggestions during the course of this work, and also to Dr. Torao Tanaka for his advice in regard to computations of ocean loading effects on tidal strain analyses.

The author also wishes to thank to Mr. Masakuni Hashida of Kyoto University for his help in installation of instruments and for his comments on tidal strain analyses.

Thanks are also due to Mr. Masaru Yamada and to Mr. Akio Hirono for their help in installation and maintenance of instruments.

The computations involved were made at the Computing Center of the Institute for Chemical Research, Kyoto University.

References

1) Blayney, J. L. and R. Gilman: A portable strain meter with continuous interferometric calibration, Bull. Seism. Soc. Amer., Vol. 55, 1965, pp. 955–970.
2) Hade, G., M. Conner and J. T. Kuo: Laser interferometer calibration system for extensometers, Bull. Seism. Soc. Amer., Vol. 58, 1968, pp. 1379–1383.
3) Smookler, S. and J. V. Kline: Interferometric calibration of a strainmeter transducer, Bull. Seism. Soc. Amer., Vol. 61, 1971, pp. 937–955.
4) Takemoto, S.: Calibration of extensometers and strain seismometers with a laser interferometer (2), Annuals Disas. Prev. Res. Inst., Kyoto Univ., No. 16B, 1973, pp. 11–15.
5) Takemoto, S.: On calibration of "roller" extensometers with a laser interferometer, J. Geodetic Soc. Japan, Vol. 21, 1975, pp. 81–90.
6) Van Veen, H. J., J. Savino and L. E. Alsop: An optical maser strainmeter, J. Geophys. Res., Vol. 71, 1966, pp. 5478–5479.
7) Vali, V. and R. C. Bostrom: One thousand meter laser interferometer, Rev. Scient. Instr., Vol. 39, 1969, pp. 1304–1306.
8) Berger, J. and R. H. Lovberg: A laser earth strain meter, Rev. Scient. Instr., Vol. 40, 1969, pp. 1569–1575.
9) Levine, J. and J. L. Hall: Design and operation of a methane absorption stabilized laser strainmeter, J. Geophys. Res., Vol. 77, 1972, pp. 2595–2609.
10) Goulty, N. R., G. C. P. King and A. J. Wallard: Iodine stabilized laser strainmeter, Geophys. J. R. astr. Soc., Vol. 39, 1974, pp. 269–282.
11) Pertzev, B. P.: The calculation of zero point drift during observation on elastic tides, Izv. Acad. Sc. USSR Ser. Geophys., 1959, pp. 547–548.
12) Furuzawa, T., S. Takemoto and K. Onoue: Electro-optical distance measurement in Kinki, Chugoku and Shikoku districts (1974–1978), J. Geodetic Soc. Japan, Vol. 24, 1978, pp. 132–140.
13) Sydenhan, P. H.: 2000 hr comparison of 10 m quartz-tube and quartz-catenary tidal strainmeters, Geophys. J. R. astr. Soc., Vol. 38, 1974, pp. 377–387.
14) Farrell, W. E.: Deformation of the earth by surface loads, Rev. Geophys. and Space Phys., Vol. 10, 1972, pp. 761–797.
15) Ogura, S.: The tides in the seas adjacent to Japan, Bull. Hydrograph. Dep., Vol. 7, 1933.
16) Navy, Ministry of Defence, USSR: *АТЛАС ОКЕАНОВ*, Pacific Ocean, 1974.
17) Navy, Ministry of Defence, USSR: *АТЛАС ОКЕАНОВ*, Atlantic and Indian Oceans, 1977.
18) Latynina, L. A. and C. D. Rizaeva: About variations of tidal deformations before earthquakes, Izv. Acad. Sc. USSR Earth Phys., 1973, pp. 84–87.
19) Latynina, L. A. and G. I. Aksenovich: About tidal deformations at the Targer station, Tidal deformations of the earth, Nauka, Moscow, 1975, pp. 97–103.
20) Latynina, L. A. and T. P. Shishkina: About intensity of tidal and tectonic motions in the zone of the Surhob fault, Izv. Acad. Sc. USSR Earth Phys., 1978, pp. 87–93.
21) Mikumo, T., M. Kato, H. Doi, Y. Wada, T. Tanaka, R. Shichi and A. Yamamoto: Possibility of temporal variations in earth tidal strain amplitudes associated with major earthquakes, J. Phys. Earth, Vol. 25, suppl., 1977, pp. S123–S136.
22) Pertzev, B. P.: Harmonic analysis of elastic tides, Izv. Acad. Sc. USSR Ser. Geophys., 1958, pp. 946–958.